

Pressure-Induced Transport of DNA Confined in Narrow Capillary Channels

Xiayan Wang,[†] Lei Liu,[†] Qiaosheng Pu,[‡] Zaifang Zhu,[§] Guangsheng Guo,^{*,†} Hui Zhong,[⊥] and Shaorong Liu^{*,§}

[†]Department of Chemistry and Chemical Engineering, Beijing University of Technology, Beijing 100124, China

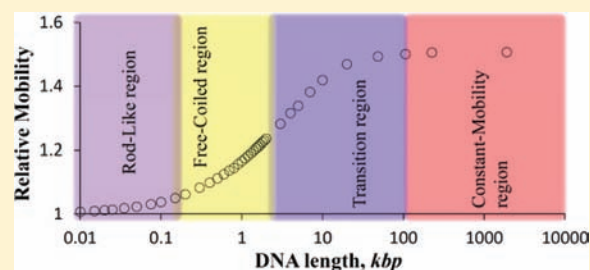
[‡]Department of Chemistry, Lanzhou University, Lanzhou, Gansu, 730000, China

[§]Department of Chemistry and Biochemistry, University of Oklahoma, Norman, Oklahoma 73019, United States

[⊥]School of Chemistry and Chemical Engineering, Huaiyin Normal University, Huaian 223300, China

Supporting Information

ABSTRACT: Pressure-induced transport of double-stranded DNA (dsDNA) from 10 base pairs (bp) to 1.9 mega base pairs (Mbp) confined in a 750-nm-radius capillary was studied using a hydrodynamic chromatographic technique and four distinct length regions (rod-like, free-coiled, constant mobility, and transition regions) were observed. The transport behavior varied closely with region changes. The rod-like region consisted of DNA shorter than the persistence length (~ 150 bp) of dsDNA, and these molecules behaved like polymer rods. Free-coiled region consisted of DNA from ~ 150 bp to ~ 2 kilo base pairs (kbp), and the effective hydrodynamic radius R_{HD} of these DNA scaled to $L^{0.5}$ (L is the DNA length in kbp), a characteristic property of freely coiled polymers. Constant mobility region consisted of DNA longer than ~ 100 kbp, and these DNA had a constant hydrodynamic mobility and could not be resolved. Transition region existed between free-coiled and constant mobility regions. The transport mechanism of DNA in this region was complicated, and a general empirical equation was established to relate the mobility with DNA length. Understanding of the fundamental principles of DNA transport in narrow capillary channels will be of great interest in the development of “lab-on-chip” technologies and nongel DNA separations.



INTRODUCTION

Manipulating and separating DNA and other large biomolecules within a micro/nanofluidic channel are of crucial importance to “lab-on-chip” (LOC) technologies for bioanalysis. As the dimensions of a fluidic channel approach the size of a DNA molecule, the transport properties of the DNA may change considerably because the effects of finite molecular size can dominate under these conditions. These property changes have led to ground-breaking discoveries and applications. For example, DNA confinement effects have been utilized in novel diagnostic assays, such as DNA entropic traps,¹ solid-state nanopores,^{2–5} and artificial sieving structures.^{6–10} These advances stress the importance of understanding the transport of DNA in narrow channels^{11–16} that underlie current and future LOC technologies.

DNA separations are usually carried out by gel electrophoresis, which utilizes viscous polymer matrices and high-electric fields. While gels can be problematic (especially when the separations are performed using narrow capillaries and microchannels), high-electric fields are incompatible with the most-commonly used silicon substrates. The pressure-induced size-dependent transport of DNA confined in a narrow capillary channel could potentially allow DNA separations to be performed on a silicon LOC device without gels or high-

electric fields, which would have a great impact on LOC technologies since fabrication methods for complex and multidimensional structures on silicon chips already exist.

In this work, we use a hydrodynamic chromatographic (HDC) technique to study the fundamental mechanisms of pressure-induced transport of DNA ranging from 10 bp to 1.9 Mbp confined in a 750 nm radius bare capillary. Based on the mobility changes, we identify four distinct size regions as presented in Figure 1, and we utilize an HDC quadratic model to study their transport mechanisms.

EXPERIMENTAL SECTION

Materials and Reagents. GeneRuler ultra low range DNA ladder was from Fermentas Life Sciences Inc. (Glen Burnie, MD). A 100 bp ladder was obtained from Amersham Biosciences (Piscataway, NJ). A 1-kbp DNA ladder, yeast chromosome PFG marker and β -agarase I were bought from New England Biolabs (Ipswich, MA). Tris-(hydroxymethyl)-aminomethane (Tris), ethylenediaminetetraacetic acid (EDTA), and sodium hydroxide were purchased from Fisher Scientific (Fisher, PA). YOYO-1 was obtained from Molecular Probes (Eugene, OR). Fused-silica capillaries (750 nm radius) were specially produced by Polymicro Technologies (Phoenix, AZ). All solutions

Received: December 19, 2011

Published: April 18, 2012

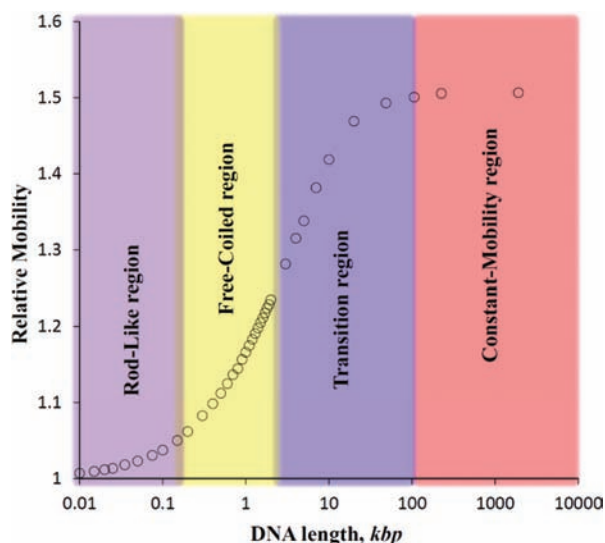


Figure 1. General relationship between DNA relative mobility and its size. The circles represent the mobilities of DNA in a 750 nm radius capillary channel.

were prepared using ultrapure water (Nanopure ultrapure water system, Barnstead, Dubuque, IA) filtered through a 0.22 μm filter (VWR, TX) and were vacuum-degassed before use.

Apparatus. The experimental setup has been described previously.¹⁷ It consisted of a narrow capillary, a pressure chamber, and a confocal laser-induced fluorescence (LIF) detector. The sampling end of the capillary can be inserted through the septum into a solution vial inside the pressure chamber for sample injection or elution. Regulated helium gas pressure maintains the chamber pressure. The detection end of the capillary was affixed to a holder which was attached to an x - y - z translation stage to align the capillary with the LIF detector. A 488 nm beam from an argon ion laser (LaserPhysics, Salt Lake City, UT) was reflected by a dichroic mirror (Q505LP, Chroma Technology, Rockingham, VT) and focused onto the capillary through an objective lens (20 \times and 0.5 NA, Rolyn Optics, Covina, CA). Fluorescence from the capillary was collimated by the same objective lens and collected by a photosensor module (HS784-04, Hamamatsu, Japan) after passing through the dichroic mirror, an interference band-pass filter (532 nm, Carlsbad, CA), a focal lens, and a 1 mm pinhole. The gain of the photosensor (control voltage 0.9 V) was ~ 75 V/nW. The detector output was acquired by DAQCard-6062E (National Instruments, Austin, TX) and processed by an in-house program written in Labview. Our early papers^{17–20} give more details of the LIF detector and execution of bare narrow capillary–open tubular chromatography (BaNC–OTC).

Preparation of DNA Samples. The dsDNA samples were obtained by mixing the DNA with YOYO-1 (a fluorescent intercalating dye) at a dye-to-base pair ratio of $\sim 1:10$ in 1 \times TE buffer. The 106 kbp linearized bacterial artificial chromosome (BAC) DNA was prepared from the *Arabidopsis* BAC clone T6H20. A yeast chromosome PFG marker in Agarose gel was digested by β -agarase I. The dsDNA samples were freshly prepared right before use.

RESULTS AND DISCUSSION

To measure the relative mobility of a DNA, we first ran an HDC separation of a mixture of fragments and obtained a chromatogram. The velocity of each fragment was directly calculated from the effective length of the separation capillary divided by its retention time. Under the same experimental conditions, the flow rate of the mobile phase was measured (see Supporting Information for details) and converted to linear velocity. The relative mobility of a DNA was computed by dividing its velocity by the mobile phase velocity. Figure 1

presents the relative mobility of DNA from 10 bp to 1.9 Mbp in a 750 nm radius capillary.

An electrostatic interaction mechanism had been proposed to explain the separations of ionic compounds in narrow capillaries.^{18,19} While it worked well for small ions, it could not explain the high resolutions of large DNA molecules.²¹ We then discovered that the DNA relative mobility could be nicely fitted with the HDC quadratic model.

Figure 2a presents a schematic illustration of the HDC model. When two particles with radii of p and q inside a

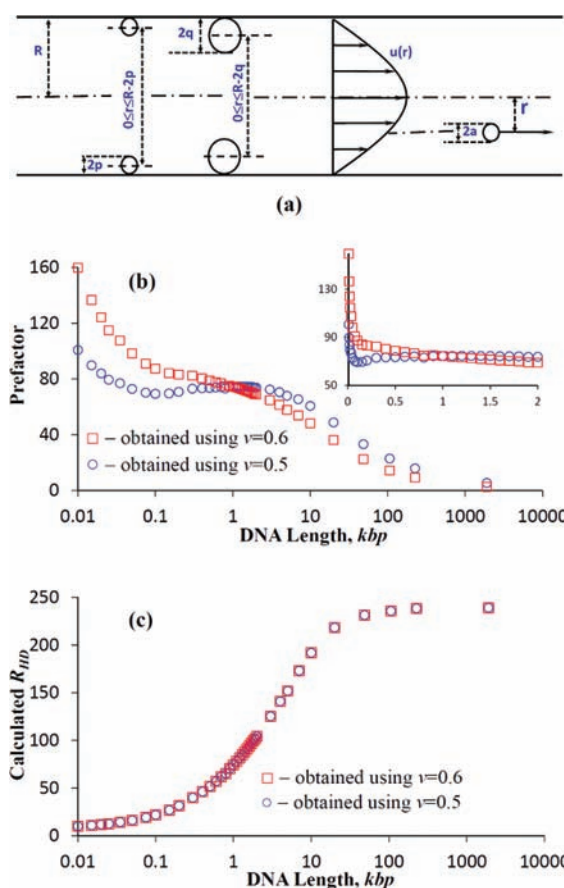


Figure 2. (a) Schematic illustration of HDC mechanism. (b) Prefactor as a function of L . (c) Calculated R_{HD} as a function of L .

capillary are carried by Poiseuille flow, the larger particle will move faster than the smaller one because the former is excluded from the wall ($R - q \leq r \leq R$) where the flow is slower. If we assume: (1) the particle is small enough to not affect laminar flow around it, (2) Brownian motion takes place in all possible radial directions in the capillary cross-section, and (3) the radial diffusion for this particle size class and capillary radius is rapid enough to transport the particle over the column cross-section many times within the total residence time such that its velocity can be expressed as the average of all stream lines that are accessible to it in the cross-section,²² then

$$\bar{u}_a = 2\pi \int_0^{R-a} u(r) \cdot r dr = \bar{u}(1 + 2\lambda - \lambda^2) \text{ or}$$

$$\bar{\mu}_a = \frac{\bar{u}_a}{\bar{u}} = (1 + 2\lambda - \lambda^2) \quad (1)$$

where $u(r)$ represents the velocity profile of a Poiseuille flow, a is the radius of the particle, $\lambda = a/R$, \bar{u} is the average velocity of the eluent, and $\bar{\mu}_a = \bar{u}_a/\bar{u}$ is the relative mobility of the particle—a parameter that is independent of pressure gradient. Equation 1 is the HDC quadratic model.

According to the literature,²² a macromolecule can be treated as a virtual particle having an effective hydrodynamic radius of R_{HD} , and

$$R_{\text{HD}} = c \times L^\nu \quad (2)$$

where L is the molecular size in kbp, ν is the scaling exponent, and c is a prefactor. After a is replaced by R_{HD} , eq 1 changes to

$$\bar{\mu}_a = \frac{\bar{u}_a}{\bar{u}} = 1 + 2 \times \frac{c \times L^\nu}{R} - \left(\frac{c \times L^\nu}{R} \right)^2 \quad (3)$$

Various values of ν have been obtained for dsDNA.^{23,24} Often, $\nu = 0.6$ for self-avoiding persistent polymers,^{16,25,26} and $\nu = 0.5$ for ideal nonself-avoiding polymers.²⁷

Using $\nu = 0.5$ (or 0.6) and $R = 750$ nm, we used eq 3 to calculate the prefactor value of every DNA fragment with its relative mobility data exhibited in Figure 1. These results are presented in Figure 2b. Figure 2c presents the calculated R_{HD} ($= c \times L^\nu$) as a function of L . Based on these data, we observed four distinct regions. Referring to Figure 2b, we see two turning points: one at ~ 100 – 200 bp and the other at ~ 2 kbp. We termed the first group of DNA [consisting of DNA shorter than the persistence length (~ 150 bp) of dsDNA] the rod-like region, and the second group of DNA (from ~ 150 bp to 2 kbp) the free-coiled region. Referring to Figure 2c, the calculated R_{HD} of DNA longer than ~ 100 kbp was a constant, and this group of DNA was called the constant mobility region. The gap between free-coiled and constant mobility regions was called the transition region.

Rod-Like Region. For a dsDNA, it has a persistence length of ~ 150 bp. Fragments shorter than this length will behave like molecular rods. According to Smith et al.,²⁸ the scaling exponent is expected to increase for these “semiflexible” molecules. The rapidly decreasing prefactor (see inset of Figure 2b) is an indication that the predetermined scaling exponent was too small. To acquire the appropriate scaling exponent value, we separated a GeneRuler ultra low range DNA ladder which contained 11 fragments from 10 to 300 bp, and the chromatogram is presented in Figure 3a. When the relative mobility data were best-fitted with eq 3, we obtained $\nu = 0.728$, and $c = 76$ nm kbp $^{-0.728}$. The fitting also produced an excellent correlation coefficient ($r^2 = 0.9999$). This scaling exponent number is greater than the previous reported value ($\nu = 0.68$),²⁹ presumably because the fragments we tested in this work were shorter than those tested in the literature.

Free-Coiled Region. Referring to the inset of Figure 2b, the prefactor did not change much as L increased from ~ 150 bp to ~ 2 kbp, especially for the data calculated using $\nu = 0.5$. That is, R_{HD} scales to $L^{0.5}$, a characteristic property for freely coiled polymers.

To examine these data in details, we present an HDC chromatogram (Figure 4a) of a 100 bp DNA ladder. When the relative mobility data were best-fitted with eq 3 (see Figure 4b), it generated: $\nu = 0.5$, $c = 75$ nm kbp $^{-0.5}$, and $r^2 = 0.9997$. The prefactor value is in good agreement with the reported number for dye-intercalated DNA.¹⁶ If we use $\nu = 0.6$ for the fitting, the relatively poor fitting results ($r^2 = 0.9981$ with $c = 60$ nm kbp $^{-0.6}$) were obtained, indicating that the scaling exponent

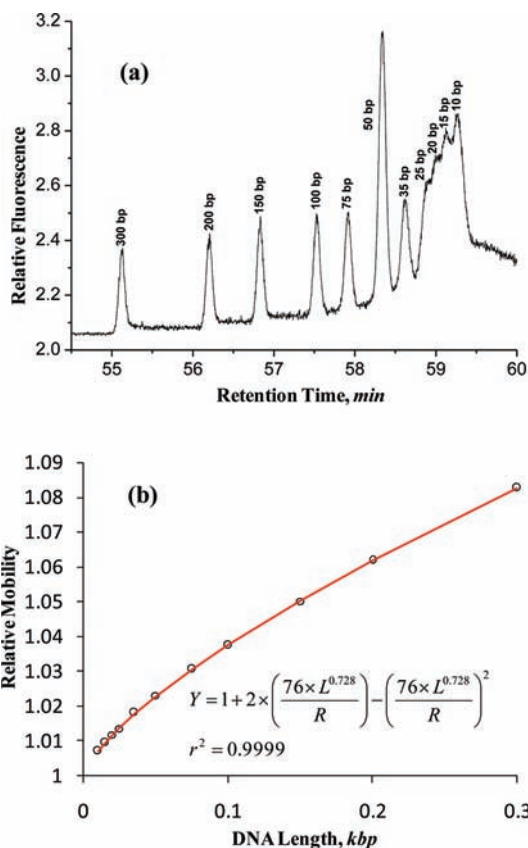


Figure 3. Separation of a GeneRuler ultra low range DNA ladder. (a) Chromatogram. (b) The fitting result. The sample contained 60 ng of total DNA/ μL . The eluent contained 10 mM TE. The capillary had a radius of 750 nm and a total length of 100 cm (95 cm effective). The sample was injected at 100 psi for 10 s, and the separation was carried out at 500 psi.

value was closer to 0.5 than to 0.6. If we included data points of DNA longer than 2 kbp for the fitting, the correlation coefficient was reduced. Therefore, the limits of free-coiled region were determined to be from ~ 150 bp to 2 kbp.

Constant Mobility Region. DNA from 106 kbp to 1.9 Mbp could not be resolved using a 750 nm radius capillary. Therefore, these fragments had a similar relative mobility. Using $R_{\text{HD}} = 75 \times L^{0.5}$ (suitable for freely coiled DNA), we have $R_{\text{HD}} = 772$ nm for the 106 kbp fragment and $R_{\text{HD}} = 3.2$ μm for the 1.9 Mbp fragment. As the freely coiled R_{HD} was greater than R , a DNA had to deform itself, yielding a cylindrical shape, to fit the bore of the narrow capillary. The cylindrical DNA should occupy the “entire” cross-section of the capillary bore. Increasing L would increase the length of the DNA cylinder but not its cross-section. Since HDC mobility is a function of the effective radius of the cross-section, not the dimension parallel to the flow streaming line, constant mobility region was observed. Constant mobility region is similar to the biased reptation in gel electrophoresis.³⁰

In the above discussion, we stated that the DNA occupied the “entire” cross-section of the capillary bore. Because the DNA molecule was very “porous”, its R_{HD} was much smaller than R . The experimental data indicated that the R_{HD} of a DNA in constant mobility region was ~ 240 nm (see Figure 2c), approximately one-third of the capillary radius—750 nm. In the Supporting Information, we included a video showing the transport of λ DNA confined in a 1 μm radius capillary. In this

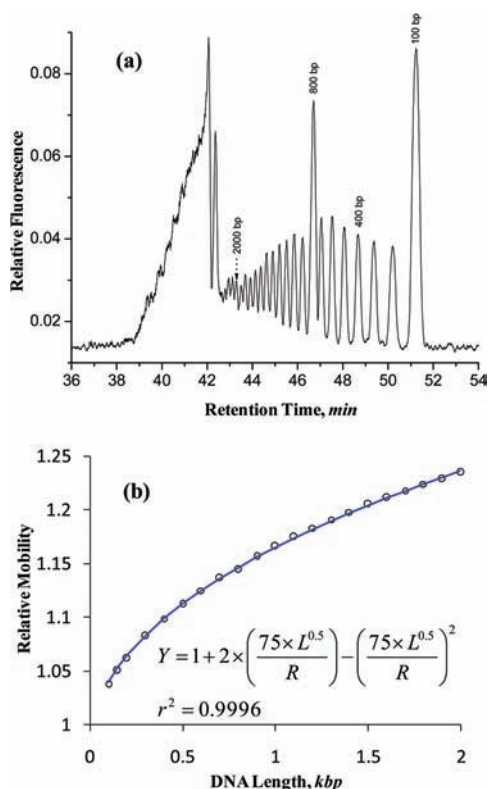


Figure 4. Separation of a 100 bp DNA ladder. (a) Chromatogram. (b) The fitting result. The sample contained 60 ng of total DNA/ μL . The eluent contained 10 mM TE. The separation capillary had a radius of 750 nm and a total length of 46 cm (42 cm effective). The sample was injected at 100 psi for 10 s, and the separation was carried out at 90 psi.

video, we see that λ DNA molecules were stretched along the axis of the capillary and that these molecules stayed preferentially in the middle of the capillary.

Transition Region. Between free-coiled and constant mobility regions, there was a gap (from ~ 2 to ~ 100 kbp). The gap is best understood as a “transition zone”. The relative mobility of DNA in this region could not be fitted well with eq 3. Several factors may be attributed to the deviations from the HDC model: (1) DNA getting stretched to cylindrical shapes when present in a space-confining narrow capillary, (2) DNA blocking (more accurately, averaging) the local flow, and (3) DNA radial motion.^{31,32} In a narrow capillary, a long DNA could be deformed, forming an elongated cylindrical shape (see the video in Supporting Information). This effect reduced the effective radius of the molecule in the HDC model and therefore decreased the relative mobility of the DNA. As an analyte occupies a significant portion of the radial capillary cross section, it blocks the stream lines of the occupied area. Because the molecule must move as an intact entity, its velocity is approximately the average of the residual stream lines. Obviously, net moving speed is also decreased. On the other hand, the radial motion forces the DNA toward the center of the capillary, which makes the DNA move faster.

It is challenging to find a simple analytical expression that takes into account all the above effects. Interestingly, we noticed that the difference between the measured mobility and eq 3 fitted mobility changed proportionally with L . We then modified eq 3 by simply adding a term kL (where k is a constant) to the right-side of the equation. To test whether we

could use this modified equation to fit the mobility data, we present a chromatogram (see Figure 5a) of a GeneRuler 1 kb

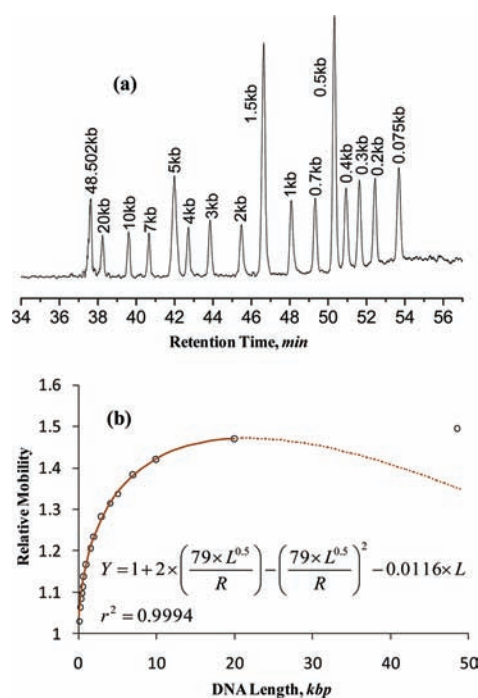


Figure 5. Separation of a mixture of GeneRuler 1 kb plus DNA ladder and λ DNA. (a) Chromatogram. (b) The fitting result. The sample contained 60 ng of total DNA/ μL . The eluent contained 10 mM TE. The separation capillary had a radius of 750 nm and a total length of 50 cm (45 cm effective). The sample was injected at 100 psi for 10 s, and the separation was carried out at 100 psi.

plus DNA ladder and λ DNA. Figure 5b presents the fitted results from 2 to 20 kbp. The good correlation coefficient ($r^2 = 0.9994$) indicates that the modified equation worked satisfactorily.

It is worth pointing out that studies on pressure-driven transport of DNA confined in narrow fluidic channels were pioneered by Stein et al.³³ using fluorescence microscopy. To measure the DNA mobility, these investigators selected three DNA (8.8, 20.3, and 48.5 kbp) and allowed a solution containing one of the DNA to flow through a slit-channel continuously under a constant pressure. The trajectories of individual DNA molecules inside the channel were recorded using a CCD camera at a frame rate of 5 Hz. The relative mobility of a DNA was calculated by averaging its trajectory velocities divided by the velocity of the 48.5 kbp DNA. On the basis of these relative mobility data, these investigators observed two distinct regimes (in terms of channel depth): in deep channels the mobility of DNA increased with molecular length, and in shallow channels all DNA had a constant mobility. These regimes are actually corresponding to transition and constant mobility regions we observed in this work. Stein et al.³³ could not observe the other two (rod-like and free-coiled) regions, possibly because they did not test short oligonucleotides.

CONCLUSIONS

On the basis of varying transport behavior of DNA confined in a 750 nm radius capillary, we have identified four distinct size regions. Utilizing an HDC quadratic model, we have studied

the transport behavior and found proper equations (models) to estimate the mobility of DNA in all these regions.

The region limits have been determined using data from 750 nm radius capillaries. Obviously, these limits will change with capillary radius. To confirm this, we performed a separation of a GeneRuler 1 kb plus DNA ladder, a λ DNA monocut mix, and a 106 kbp fragment using a 2.5 μm radius capillary (see Figure 6a). Figure 6b presents the fitted results using eq 3, and Figure 6c presents the fitted results using the modified equation. These results revealed that the limits of free-coiled region was

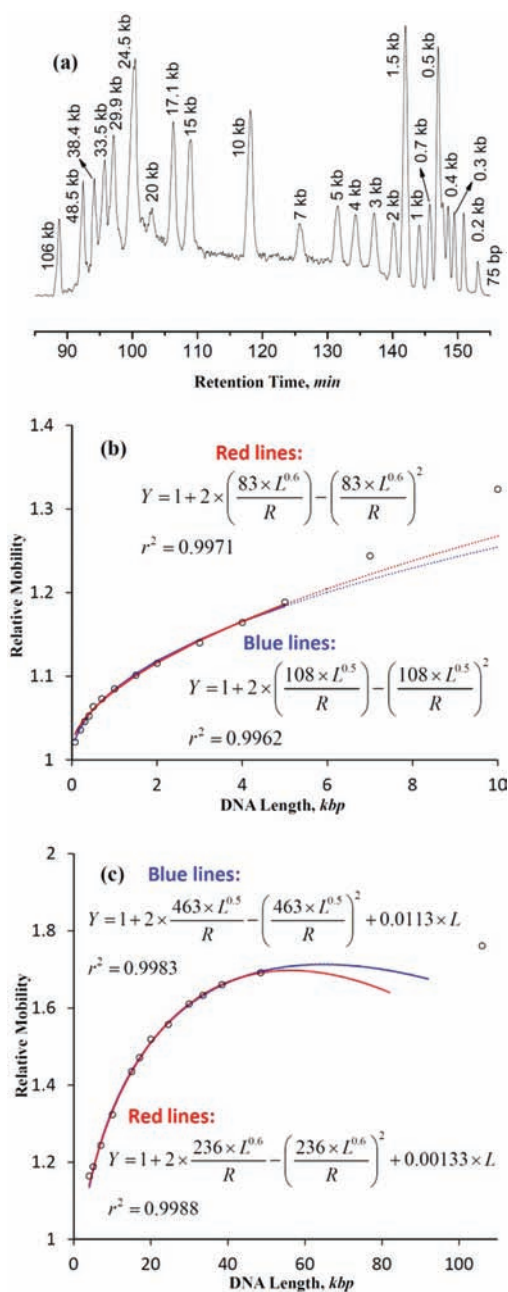


Figure 6. Separation of DNA mixture. (a) Chromatogram. (b) The fitting results. Sample: a mixture of 25 ng/ μL linearized T6H20 BAC DNA, 25 ng/ μL λ DNA mono cut mix, and 25 ng/ μL GeneRuler 1 kb plus DNA ladder. The eluent contained 10 mM TE. The separation capillary had a radius of 2.5 μm and a total length of 445 cm (440 cm effective). The sample was injected at 100 psi for 10 s, and the separation was carried out at 360 psi.

widened from ~ 200 bp to ~ 5 kbp, and the limits of transition region was shifted to longer DNA (~ 5 to >106 kbp). It also revealed that either $\nu = 0.5$ or 0.6 could be used to fit the mobility data. In a separate experiment, the yeast DNA could not be separated in a 750 nm radius capillary, but they were partially resolved in a 5 μm radius capillary (data not shown). Such larger radius capillaries exhibit reduced resolutions for short DNA fragments, however. The use of both narrow and relatively wider capillaries could solve this problem.

■ ASSOCIATED CONTENT

Supporting Information

Experimental setup, scanning electron microscopy image, and supplemental data; preparation of BAC DNA and restriction digestion; measurement of eluent flow rate; and video showing the transport of λ DNA confined in 1 μm radius capillary. These materials are available free of charge via the Internet at <http://pubs.acs.org>.

■ AUTHOR INFORMATION

Corresponding Author

guogs@bjut.edu.cn; shaorong.liu@ou.edu

Notes

The authors declare no competing financial interest.

■ ACKNOWLEDGMENTS

This work was supported by the National Science Foundation (CHE 1011957), National Science Foundation of China (20935002, 21075006, 20975043), and Beijing Natural Science Foundation (2112003).

■ REFERENCES

- (1) Han, J.; Craighead, H. G. *Science* **2000**, *288*, 1026.
- (2) Li, J.; Stein, D.; McMullan, C.; Branton, D.; Aziz, M. J.; Golovchenko, J. A. *Nature* **2001**, *412*, 166.
- (3) Storm, A. J.; Chen, J. H.; Ling, X. S.; Zandbergen, H. W.; Dekker, C. *Nat. Mater.* **2003**, *2*, 537.
- (4) Iqbal, S. M.; Akin, D.; Bashir, R. *Nature Nanotechnol.* **2007**, *2*, 243.
- (5) van Drop, S.; Keyser, U. F.; Dekker, N. H.; Dekker, C.; Lemay, S. G. *Nat. Phys.* **2009**, *5*, 347.
- (6) Volkmuth, W. D.; Austin, R. H. *Nature* **1992**, *358*, 600.
- (7) Huang, L. R.; Tegenfeldt, J. O.; Kraeft, J. J.; Sturm, J. C.; Austin, R. H.; Cox, E. C. *Nat. Biotechnol.* **2002**, *20*, 1048.
- (8) Cross, J. D.; Strychalski, E. A.; Craighead, H. G. *J. Appl. Phys.* **2007**, *102*, 024701.
- (9) Yasui, T.; Kaji, N.; Ogawa, R.; Hashioka, S.; Tokeshi, M.; Horiike, Y.; Baba, Y. *Anal. Chem.* **2011**, *83*, 6635.
- (10) Strychalski, E. A.; Lau, H. W.; Archer, L. A. *J. Appl. Phys.* **2009**, *106*, 024915.
- (11) Perkins, T. T.; Smith, D. E.; Chu, S. *Science* **1997**, *276*, 2016.
- (12) Smith, D. E.; Chu, S. *Science* **1998**, *281*, 1335.
- (13) Smith, D. E.; Babcock, H. P.; Chu, S. *Science* **1999**, *283*, 1724.
- (14) Schroeder, C. M.; Babcock, H. P.; Shaqfeh, E. S. G.; Chu, S. *Science* **2003**, *301*, 1515.
- (15) Quake, S. R.; Babcock, H.; Chu, S. *Nature* **1997**, *388*, 151.
- (16) Tegenfeldt, J. O.; Prinz, C.; Cao, H.; Chou, S.; Reisner, W. W.; Riehn, R.; Wang, Y. M.; Cox, E. C.; Sturm, J. C.; Silberzan, P.; Austin, R. H. *Proc. Natl. Acad. Sci. U.S.A.* **2004**, *101*, 10979.
- (17) Wang, X.; Cheng, C.; Wang, S.; Zhao, M.; Dasgupta, P. K.; Liu, S. *Anal. Chem.* **2009**, *81*, 7428.
- (18) Wang, X.; Kang, J.; Wang, S.; Lu, J. J.; Liu, S. *J. Chromatogr., A* **2008**, *1200*, 108.
- (19) Wang, X.; Wang, S.; Veerappan, V.; Byun, C.; Nguyen, H.; Gendhar, B.; Allen, R. D.; Liu, S. *Anal. Chem.* **2008**, *80*, 5583.

- (20) Wang, X.; Veerappan, V.; Cheng, C.; Jiang, X.; Allen, R. D.; Dasgupta, P. K.; Liu, S. *J. Am. Chem. Soc.* **2010**, *132*, 40.
- (21) Wang, X.; Liu, L.; Wang, W.; Pu, Q.; Guo, G.; Dasgupta, P. K.; Liu, S. *Trends Anal. Chem.* **2012**, *35*, 122.
- (22) Tijssen, R.; Bos, J.; van Kreveld, M. E. *Anal. Chem.* **1986**, *58*, 3036.
- (23) Duval, M.; Lutz, P.; Strazielle, C. *Makromol. Chem. Rapid Commun.* **1985**, *6*, 71.
- (24) Hodgson, D. F.; Amis, E. J. *J. Chem. Phys.* **1991**, *95*, 7653.
- (25) Flory, P. J. *Principles of Polymer Chemistry*; Cornell University Press: Ithaca, NY, 1953.
- (26) Schaefer, D. W.; Joanny, J. F.; Pincus, P. *Macromolecules* **1980**, *13*, 1280.
- (27) Dobay, A.; Dubocher, J.; Millett, K.; Sottas, P.-E.; Stasiak, A. *Proc. Natl. Acad. Sci. U.S.A.* **2003**, *100*, 5611.
- (28) Smith, D. E.; Perkins, T. T.; Chu, S. *Macromolecules* **1996**, *29*, 1372.
- (29) Sorlie, S.; Pecora, R. *Macromolecules* **1990**, *23*, 487.
- (30) Slater, G. W.; Noolandi, J. *Biopolymers* **1989**, *28*, 1781.
- (31) Shafer, R. H.; Laiken, N.; Zimm, B. H. *Biophys. Chem.* **1974**, *2*, 180.
- (32) Shafer, R. H. *Biophys. Chem.* **1974**, *2*, 185.
- (33) Stein, D.; van der Heyden, F. H. J.; Koopmans, W. J. A.; Dekker, C. *Proc. Natl. Acad. Sci. U.S.A.* **2006**, *103*, 15853.